Original article

Physicochemical, pharmacokinetics, and histological evaluation of new naproxen-quercetin co-lyophilizate to diminish drug-induced gastric irritations in rats

Mohamed Abbas Ibrahim [a,b,*], Gamal A. Shazly [a,c], Gehan M. Elossaily [d,e], Essam Ezzeldin [f,g], Fadilah S. Aleanizy [a]

[a] Department of Pharmaceutics, College of Pharmacy, King Saud University, PO Box 2457, Riyadh 11451, Saudi Arabia
[b] Department of Pharmaceutics and Industrial Pharmacy, Faculty of Pharmacy, Al-Azhar University, Assiut, Egypt
[c] Department of Industrial Pharmacy, Faculty of Pharmacy, Assiut University, Assiut, Egypt
[d] Department of Pathology, Faculty of Medicine, Almareffa College for Science and Technology, Riyadh, Saudi Arabia
[e] Department of Pathology, Faculty of Medicine, Assiut University, Assiut, Egypt
[f] Department of Pharmaceutical Chemistry and Drug Bioavailability Laboratory, College of Pharmacy, King Saud University, Saudi Arabia
[g] Drug Bioavailability Center, National Organization for Drug Control and Research, (NODCAR), Cairo, Egypt

ABSTRACT

Quercetin (QUE) is a flavonoid found in several plants and commonly distributed in edible vegetables and fruits. To evaluate the effect of co-lyophilization of naproxen (NPX) with QUE at different weight ratios on physicochemical characteristics induced gastric irritation, and drug pharmacokinetics. NPX binary systems with QUE in different weight ratios were prepared by freeze-drying alkalinized solutions, and were characterized in terms of physicochemical properties as well as NPX dissolution rate in acidic pH. NPX-induced gastric inflammation studies were carried out in rats for 7 days. The pharmacokinetics of the two formulations were assessed to evaluate the bioavailability of NPX-QUE 1:2 co-lyophilizate. Westar rats were administered oral doses equivalent to 40 mg kg^{-1} of NPX and blood samples were taken from the retro-orbital vein of rats at 0.5, 1.0, 1.5, 2.0, 3.0, 4.0, 6.0, 8.0 12.0, and 24.0 h post dosing. Co-lyophilization of NPX with QUE enhanced drug dissolution rate in the acidic medium, which was correlated with an increased QUE weight ratio in the co-lyophilizates. Rat stomachs from group V (NPX-QUE 1:2 co-lyophilizate) showed non-significant changes, and biopsies from this group showed no significant leukocyte infiltration and edema in the mucosa. The bioavailability of NPX-QUE 1: 2 co-lyophilizate was similar to the control sample. NPX-QUE 1: 2 co-lyophilizate could be an alternative to NPX in the treatment of arthritis as it minimizes the potential for gastric irritation and enhances safety while retaining the same efficacy and bioavailability.

1. Introduction

Synthetic drugs are a major component of the treatment in the management of arthritis. Conventional drug treatment of inflammatory disorders such as rheumatic arthritis is based on the use of analgesic, non-steroidal anti-inflammatory drugs (NSAIDs), disease-modifying anti-rheumatic drugs, and corticosteroids (Schuna and Megeff, 2002).

NSAIDs comprise a class of pharmaceutical active ingredients (APIs) that are extensively used for their anti-inflammatory, analgesic, and antipyretic properties (Scarpignato and Hunt, 2010). However, prolonged use of this class of drugs has been frequently related to several systemic adverse reactions, principally in the gastrointestinal (GI) tract. The mechanism underlying these NSAID-induced GI adverse reactions might be due to the accumulation of these drugs in epithelial cells during their absorption, which result in local toxicity involving the induction of mitochondrial dysfunction (Matsui et al., 2011).

In 1999, the Arthritis, Rheumatism, and Aging Medical Information System data revealed that 13 out of every 1000 patients with rheumatoid arthritis who were administered NSAIDs for 1 year suffered from serious GI problems (Dhikav et al., 2003). In addition, the rate of death associated with NSAID-related GI toxic reactions was found to be 0.22% per year, with an annual relative risk of 4.21 compared to the risk for persons not using NSAIDs (Lain, 2002). In another study examining 5526 patients treated with NSAIDs, death was found to have increased from 14.7% (range = 13.6% to 15.8%) before 1997 to 20.9% (range = 18.8% to 22.9%) since 1997 (Straube et al., 2009).

The majority of anti-inflammatory drugs lead to reactive gastropathy, which is injurious to the gastric mucosa (Matsui et al., 2011). This reactive gastropathy is also referred to as chemical gastropathy, reflux gastritis, and type C gastritis (Kayaçetin and Güreşçi, 2014). Grading of chemical gastritis measures the severity of the inflammatory lesions.

Naproxen (NPX) is an NSAID that has anti-inflammatory, antipyretic, and pain-relieving properties. NPX causes numerous adverse reactions, including gastric erosions, antral ulceration, and petechial bleeding in the mucosa (Chairmandurai et al., 2010). The mechanism underlying these NPX-induced gastric adverse reactions, similar to that of other NSAIDs, is the production of oxygen free radicals and lipid peroxidation (Ghosh et al., 2015).

Several studies have investigated different chemical compounds for use in gastric protection. Kim et al. (2005) studied the in vivo protective action of astaxanthin extracted from *Xanthophyllomyces dendrorhous* against NPX-induced gastric antral ulceration in rats. They showed that the concomitant oral administration of flavonoids exhibited a gastro-protecting and curing action against the NSAIDs-induced gastric antral ulcer and prevented the increase in the lipid peroxide level in gastric mucosa, as well as a substantial increase in the activities of radical scavenging enzymes such as superoxide dismutase, catalase, and glutathione peroxidase. The orally administered astaxanthin exhibited significant gastroprotective effects against the drug-induced gastric antral ulcer. The authors attributed this finding to the repressed elevation of the gastro-mucosal lipid peroxide level.

Quercetin (3,3′,4′,5,7-pentahydroxyflavone, QUE) is a flavonoid (polyphenol) commonly distributed in edible vegetables and fruits. Carrasco-Pozo et al. (2012a,b) reported that a polyphenol-containing herbal extract minimized indomethacin-induced oxidative stress, mitochondrial dysfunction, and cell death from in vitro and in vivo models of GI damage. They showed in a later study (Carrasco-Pozo et al., 2016) that the gastro-protective actions of QUE recorded in the rat gastric and ileal mucosa indicated that QUE might be beneficial in the prevention and/or treatment of nonsteroidal anti-inflammatory drug-associated side effects, without interfering with their therapeutic effectiveness.

In the present study, the effects of co-lyophilization of NPX with QUE of different weight ratios on the physicochemical characteristics as well as drug dissolution were investigated. Additionally, the effects of these drug-QUE co-lyophilizates on the drug-induced gastric inflammation were evaluated.

2. Materials and methods

2.1. Materials

NPX and QUE (3,3′,4′,5,7-pentahydroxyflavone) were purchased from Sigma Chemical Co. (St. Louis, MO, USA). High-performance liquid chromatography grade acetonitrile (ACN) was obtained from Avonchem Ltd. (Wellington House, Cheshire, UK). Other materials and solvents are of reagent or analytical grade, and they were used without further purification.

2.2. Methods

1. Freeze-drying of NPX-QUE binary systems (co-lyophilization)

NPX-QUE binary systems of different weight ratios (1:0.25, 1:0.5, 1:1, and 1:2) were freeze-dried. The required weights of NPX and QUE were dispersed in 20 mL distilled water using a vortex. Since NPX and QUE are poorly soluble and acidic in nature, to dissolve both ingredients, 3–5 mL of concentrated ammonia solution was added dropwise until a clear solution was formed. The resulting solutions were freeze-dried at −60 °C and the vacuum pressure was less than 1 mbar (Alpha 1-4 LD Plus, Martin Christ Gefriertrocknugs anlagen GmbH, Osterode am Harz, Germany) and stored in tightly sealed containers protected from the light until subsequent analysis.

2. NPX-QUE physical mixtures

NPX-QUE physical mixtures corresponding to the co-lyophilizates in different drug weight ratios were obtained by gently mixing the weighed amounts of NPX and QUE in a porcelain mortar.

3. Morphological characterization

A scanning electron microscope (SEM) (Zeiss EVO LS10; Cambridge, UK) was used to determine the morphological characteristics of the NPX and QUE powders, and the solid dispersion of the NPX-QUE mixtures. The samples were placed on stubs using double sided adhesive carbon tape (SPI Supplies, West Chester, USA) and covered with gold under vacuum in a Q150R sputter coater unit (Quorum Technologies Ltd., East Sussex, United Kingdom) in an atmosphere of argon for 120 s at 20 mA.

4. In vitro dissolution studies

The dissolution rates of different NPX-QUE co-lyophilizates as well as their corresponding physical mixtures were studied in triplicate using the dissolution paddle method (USP Dissolution Apparatus II; Caleva Ltd., Model 85T). The dissolution apparatus was set to 100 rpm and the temperature was maintained at 37 ± 0.5 °C. The dissolution apparatus was equipped with a continuous automated monitoring system consisting of an IBM computer PK8620 series and PU 8605/60 dissolution test software, Philips VIS/UV/NIR single beam eight cell spectrophotometer Model PU 8620, Epson FX 850 printer, and a Watson-Marlow peristaltic pump. In each flask was 500 mL of 0.1 N HCl at pH 1.2. An amount equivalent to 25 mg, NPX was added to the dissolution medium. At predetermined time intervals, absorbance was recorded automatically at 272 nm and the percentage dissolved NPX was measured as a function of time.

Dissolution efficiency after 30 min ($DE\%_{30}$) was calculated from the area under the dissolution curve at time t (measured using the trapezoidal rule) and expressed as percentage of the area of the rectangle described by 100% dissolution at the same time (Vemula and Vangala, 2014). In addition, the relative dissolution rate (RDR_{30}) was calculated by determining the amount of NPX dissolved from a particular sample and normalizing for the amount of drug dissolved from the pure drug sample over the same time interval (30 min).

5. Differential scanning calorimetry (DSC)

DSC-60 equipment (Shimadzu, Kyoto, Japan) analyzed the thermal behavior of the NPX drug and the prepared solid dispersion with QUE. Samples of 3–5 mg were placed in aluminum pans and hermetically sealed. The scanning rate was 10 °C min^{-1} over a range of 25–200 °C. Indium was the temperature and enthalpy standard that was applied.

6. Fourier transform infrared spectroscopy (FTIR)

The FTIR spectra of NPX, QUE, and their co-lyophilizates were recorded using FTIR Perkin Elmer spectrophotometer (Spectrum BX). Samples were mixed with potassium bromide (spectroscopic grade) and compressed into disks using a hydraulic press before scanning from 4000 to 600 cm^{-1}. The data were analyzed using Perkin Elmer software (Spectrum V5.3.1).

7. NPX-induced gastric inflammation

The experiments were performed according to the 'Guide for Care and Use of Laboratory Animals' and the requirements of the Institutional Animal Ethics Committee, King Saud University, Riyadh, Saudi Arabia. The NPX-induced gastric inflammation studies used healthy Wistar rats of both sexes weighing 90–120 g that had been fasting for 18 h with water available *ad libitum*. Rats were given one of the test drug dose orally, twice each day for 5 days (10 doses in total). The administered dose of NPX or NPX-QUE co-lyophilizate equivalent to 40 mg kg^{-1} in 0.5% CMC was given by an esophageal tube. The rats were equally and randomly allocated into six groups (six rats in each group) as follows: Group I: negative control, no medication; Group II: oral untreated NPX suspension; Group III: oral lyophilized NPX suspension; Group IV: oral NPX-QUE (1:0.25) co-lyophilizate suspension equivalent to NPX dose; Group V: oral NPX-QUE (1:0.5) co-lyophilizate suspension equivalent to NPX dose; and Group VI: oral NPX-QUE (1:0.25) co-lyophilizate suspension equivalent to NPX dose.

Four hours after the last administration, the animals were sacrificed by decapitation after administration of ether inhalation anesthesia and the stomach was excised immediately, cleaned with saline solution (0.9% w/v), and placed in a 10% buffered formaldehyde saline solution.

8. Gastric gross examination

At the completion of the NPX and QUE treatment, the rats were sacrificed and their stomachs were isolated and washed in ice-cold saline solution. The lesions of the gastric mucosal injury were examined by the naked eye and photographed using a digital camera, and multiple biopsies were taken.

9. Histopathological examination

Gastric biopsies were fixed at 10% buffered formaldehyde saline for 24 h. Tissue samples were washed, dehydrated with alcohol, cleared in xylene, and embedded in paraffin in a hot air oven (56 °C) for another 24 h. The paraffin blocks were sliced into sections of 5 μm thickness, mounted on glass slides, stained with hematoxylin and eosin, and examined under a light microscope. Rugge et al. (2007) proposed that grading should represent the semiquantitative assessment of the combined severity of mononuclear and granulocytic inflammation scored in both antral and oxyntic biopsy samples. Four typical signs of inflammation grades were described: 0 = No inflammation, the presence of very few leukocytes infiltration in gastric mucosa; 1 = Mild inflammation, infiltration of a few leukocytes in the upper mucosa or at the bottom of the gastric glands; 2: Moderate inflammation = a large infiltration number of leukocytes in the total mucosa; 3: Severe inflammation = infiltration of leukocytes in the majority of the total mucosa.

10. Pharmacokinetic study in rats

The pharmacokinetic experiments followed the 'Guide for Care and Use of Laboratory Animals of Laboratory Animal Centre at the College of Pharmacy at King Saud University' (Riyadh, Saudi Arabia). Male SD rats weighing 200 ± 20 g were randomly divided into two groups (n = 6). The first group received reference formulation of naproxen and the second received the new formulation of naproxen. After 10 h of fasting, rats received oral dose of naproxen (40 mg/kg). Under partial anesthesia using diethyl ether, blood (about 0.25 mL) was withdrawn from retro-orbital vein of rats at 0.5, 1.0, 1.5, 2.0, 3.0, 4.0, 6.0, 8.0, 12.0, 24.0 h post dosing. One hour post drug administration, each rat received orally 1.5 mL 0.9% saline, water and food was allowed *ad-libitum*. Plasma were separated from blood and kept in −80 °C till analysis.

A validated analytical method for the quantification of NPX in plasma described by Elsinghorst et al. (2011) was applied. NPX and IS extracted by deproteinzation by acetonitrile The plasma samples from the rats were thawed at ambient temperature. To 100 μL of plasma, 200 μL of acetonitrile containing IS (ketoprofen, 2 μg mL^{-1}) was added. After shaking by vortex, samples centrifuged 8000g at 4 °C. The supernatant was collected and 10 μL was injected into a LC MS/MS.

The ACQUITY™ UPLC system coupled to a triple-quadruple tandem mass spectrometer Micromass Quattro micro™ (Waters Corp., Milford, MA, USA) was used to analyze the NPX concentrations in the rat plasma samples. The chromatographic separation of the NPX and IS was performed on a XBridge TM BEH C_{18} column (50 × 2.1 mm, i.d., 2.5 μm; Waters, USA) maintained at a temperature of 40 °C. The mobile phase, consisted of 0.02 M ammonium acetate buffer (pH 4.0) and acetonitrile (30/70, v/v) delivered at a flow rate of 0.2 mL/min at and. The system equipped with an electrospray ionization interface was used for quantification of the NPX and IS. Detection was performed in the electrospray ionization negative mode using multiple reaction monitoring by the ion transitions of m/z 229 > 169.99 for the NPX and m/z 253.06 > 209.09 for the IS. LC-MS/MS system, and data were collected and processed using the Target Lynx™ program.

NPX pharmacokinetic parameters were calculated using WinNonlin software (Pharsight Co., Mountain View, CA, USA). The non-compartmental pharmacokinetic model was used to calculate pharmacokinetic parameters, maximum concentration (C_{max}), time to reach maximum concentration (t_{max}), area under the curve from 0 to t (AUC_{0-24}), 0-inf (AUC_{0-inf}), elimination rate constant (kel), half-life ($t_{1/2}$), and mean residence time (MRT). All values are expressed as the mean ± standard deviation (SD).

Statistical differences of the means were assumed to be significant when $P < 0.05$ by Student's unpaired *t*-test. Data are expressed as mean ± SD (n = 8). To compare the relative bioavailability between the new formulation (NPX-QUE 1:2 co-lyophilizate) and the reference compound (NPX), the relative bioavailability (F%) was evaluated using the following equation:

$$F = AUC_{test}/AUC_{reference} \times 100$$

3. Results and discussion

1. Scanning electron microscopy (SEM)

NPX-QUE co-lyophilizates at different NPX-QUE weight ratios were characterized for their shapes and surface properties by SEM images, which are displayed in Fig. 1. The untreated drug had a regular crystalline shape, whereas the lyophilized drug showed a slight decrease in the crystal size after lyophilization. No significant changes were observed in the NPX:QUE co-lyophilizate in the 1:0.25 ratio. In addition to the presence of small-sized QUE particles, the drug particle crystal size in NPX: QUE co-lyophilizate at 1:0.5 and 1:1 wt ratios appeared slightly smaller when the QUE weight ratio increased. However, at NPX:
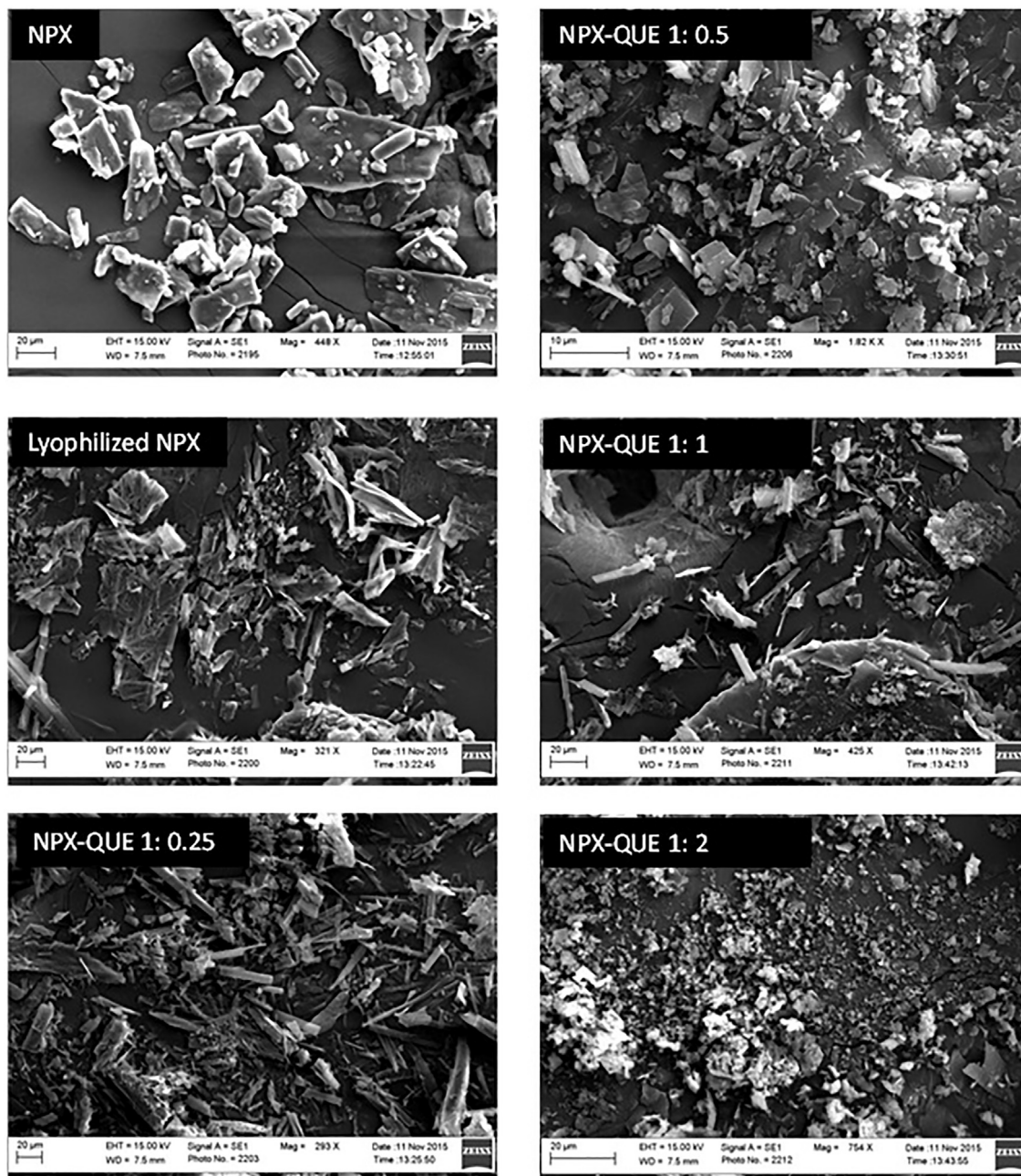
Fig. 1. Scanning electron micrographs of NPX-QUE co-lyophilizates at different weight ratios compared to the individual components.

QUE ratio of 1:2, a very pronounced decrease in both drug particle size and crystallinity was observed.

2. In vitro dissolution studies

Fig. 2 shows the *in vitro* dissolution profiles of NPX-QUE co-lyophilizates at different weight ratios compared to the untreated NPX and lyophilized NPX in acidic medium (pH 1.2). Untreated NPX exhibited very slow dissolution rates. Less than 45% of the NPX weight was dissolved within 90 min. In addition, a very slight increase in the drug dissolution rate was observed in its lyophilized form (52% dissolution after 90 min). The slow dissolution rate of both NPX and its lyophilized form might be due to its acidic nature, with solubility decreasing in acidic pH (Panahi et al., 2013).

Co-lyophilization of NPX with the flavonoid compound (QUE) resulted in a noticeable improvement in the dissolution rate. By increasing the weight ratio of QUE in the co-lyophilizates, an increased drug dissolution rate was observed. For example, the drug exhibited complete dissolution after 60 min in the NPX-QUE 1:2 co-lyophilizate, whereas only 72% of the drug was dissolved in the NPX-QUE 1:0.25 co-lyophilizate. The calculated data of the DE% after 30 min for the NPX-QUE 1:0.25 and NPX-QUE 1: 2 co-lyophilizates were 46.70% and 80.18%, respectively, whereas the drug RDR_{30} values were 5.53 and 8.43, respectively (Table 1). The dissolution profiles of NPX-QUE physical mixtures having the same weight ratios as the investigated co-lyophilizates are illustrated in Fig. 3. A very slight increase of the drug dissolution rate was observed when it was physically mixed with QUE in comparison to that observed with the corresponding co-lyophilizates (Table 1).
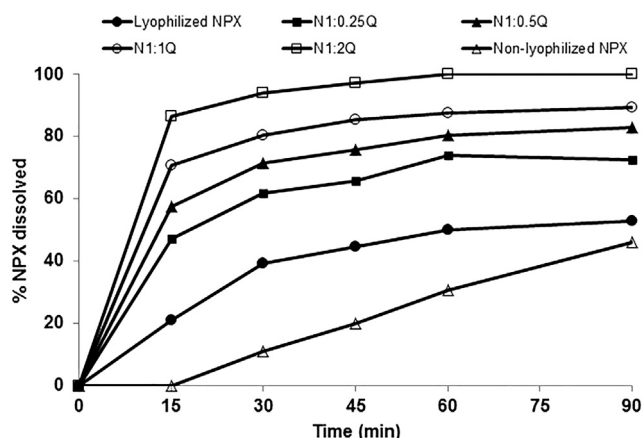
Fig. 2. Dissolution profiles of NPX -QUE co-lyophilizates at different weight ratios compared to the individual components.

Table 1
Dissolution efficiency percentages after 30 min (DE%$_{30}$) and relative dissolution rate after 30 min (RDR$_{30}$) of NPX from its-QUE binary systems[*].

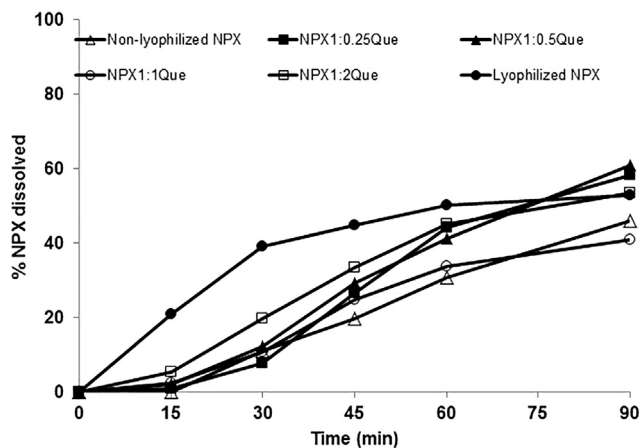| System	DE%$_{30}$	RDR$_{30}$
Non-lyophilized NPX	3.35	–
lyophilized NPX	49.61	3.52
NPX-QUE (1: 0.25) co-lyophilizate	46.70	5.53
NPX-QUE (1: 0.25) physical mix	2.83	0.69
NPX-QUE (1: 0.5) co-lyophilizate	55.93	6.41
NPX-QUE (1: 0.5) physical mix	5.05	1.11
NPX-QUE (1: 1) co-lyophilizate	66.63	7.21
NPX-QUE (1: 1) physical mix	4.69	0.97
NPX-QUE (1: 2) co-lyophilizate	80.18	8.43
NPX-QUE (1: 2) physical mix	9.24	1.77

[*] Determined at 37 °C.

Fig. 3. Dissolution profiles of NPX -QUE physical mixtures at different weight ratios compared to the individual components.

Enhancement of the NPX dissolution rate in its QUE co-lyophilizates might be due to the presence of five hydroxyl groups in the QUE molecule (Materska, 2008). These hydroxyl groups surround NPX when it is dispersed in the QUE matrix and might be attributed to the enhanced drug dissolution rate.

3. Fourier transform infrared spectroscopy (FTIR)

Fig. 4 shows the FTIR of NPX and co-lyophilizates with QUE. FTIR spectra of NPX exhibited absorption bands with characteristic peaks in the regions of 1643 cm^{-1} for the C=O, 3000 cm^{-1} for stretching of the OH, and 1592 cm^{-1} stretching of the benzene ring. The FTIR spectra of the NPX-QUE co-lyophilizates showed no evidence of disappearance or change in the characteristic absorption bands for NPX after co-lyophilization with QUE. This indicates no interaction occurred between NPX and QUE in co-lyophilizates.

4. Differential scanning calorimetry (DSC)

DSC is a beneficial technology that can measure not only the physicochemical characteristics of a drug, but also the interaction between a drug and different excipients. DSC provides information about decomposition and changes in heat capacity, melting, or crystallization of the drug. NPX exhibited a sharp endothermic peak at 157.2 °C (Fig. 5) conforming its melting point to heat of fusion 153.66 (J/g), whereas the melting point of the drug was insignificantly shifted downwards in the co-lyophilizates of the drug with QUE in all weight ratios used. This might be due to either the uniform distribution of the drug in the QUE matrix achieved via the solid dispersion preparation or the loss of NPX crystallinity.

5. Gross examination

From examination of the stomachs of the rats in the five groups, it was found that there was no evidence of macroscopic changes before ingestion of the drug in the control group (group I, Fig. 6), Marked erythema and edema in the stomachs of rats in group II and group III, and minimal erythema in group IV were observed. However, stomachs from group V showed non-significant gross changes compared to the control group. Thus, the administration of NPX in the form of co-lyophilizates with QUE had a protective role on the stomachs of rats. These results are nearly identical to those obtained by Shakeerabanu et al. (2011) who showed that QUE prevented oxidative stress and gastric damage induced by indomethacin in rats. QUE has been reported to prevent indomethacin -induced mitochondrial dysfunction via the antioxidant mechanism in Caco-2 cells (Carrasco-Pozo et al., 2012a,b). Although the study has made advances in determining the oxidative and inflammatory damage induced by indomethacin and the protective effect of polyphenolic compounds, the underlying molecular mechanisms of GI protection induced by QUE have not yet been characterized.

6. Histopathological examination

As chemical gastritis can occur in rats treated with NSAIDs, histological evaluation of the gastric mucosa is important for assessing mucosal changes. All slides were estimated by one single experienced pathologist who was blinded to the characterizations of the rats. Data were obtained from three distinct high-power fields, and their mean value was calculated. Each specimen from the five groups was examined for the presence of inflammatory cells, foveolar hyperplasia, erosions, ulceration, congestion, hemorrhagic damage, and edema in the upper mucosa and submucosa. The inflammation grades of the gastric tissue were based on semi-quantitative evaluation. Each inflammation grading result was based on an average of the grades of three high power fields under the microscope. The histological results showed that the rats in the control group showed an intact appearance of the gastric mucosal structure (grade 0). In contrast, 3 out of 5 rats and 4 rats out of 5 in groups II and III showed severe (grade 3) and moderate (grade 2) degree of inflammation, respectively, in the form of eosinophilic and neutrophilic infiltration of the lamina propria and in between mucosal glands, congested capillaries, and edema with focal mucosal erosions were detected. Four out of five rats in group IV had markedly better protection of gastric mucosa from NPX that
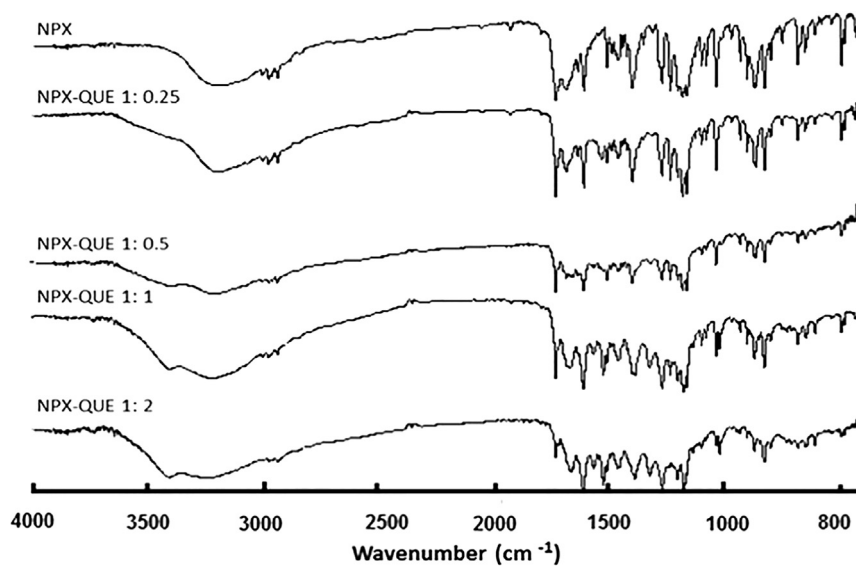
Fig. 4. IR spectra of NPX -QUE co-lyophilizates at different weight ratios compared to the individual components.
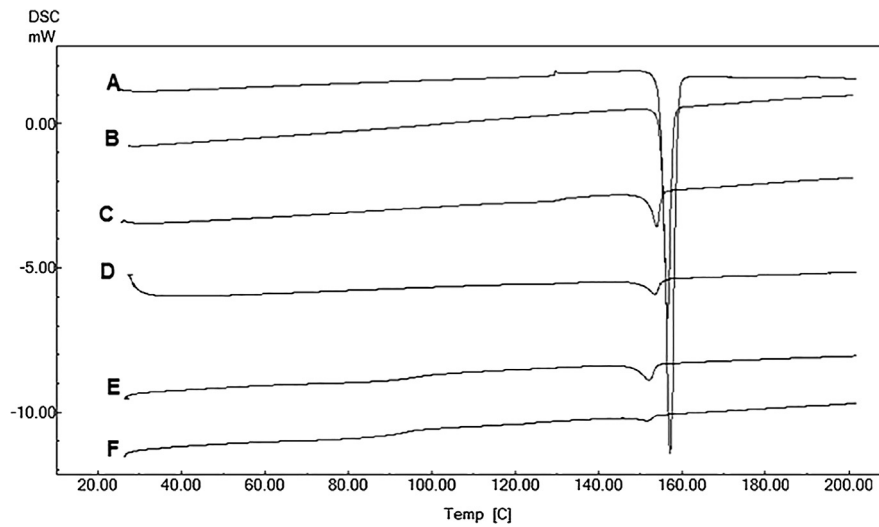

Fig. 5. DSC thermograms of NPX-QUE co-lyophilizates. A: lyophilized NPX; B: non- lyophilized NPX; C: co-lyophilized NPX-QUE (1:0.25); D: co-lyophilized NPX-QUE (1:0.5); E: co-lyophilized NPX-QUE (1:1); F: co-lyophilized NPX-QUE (1:2).
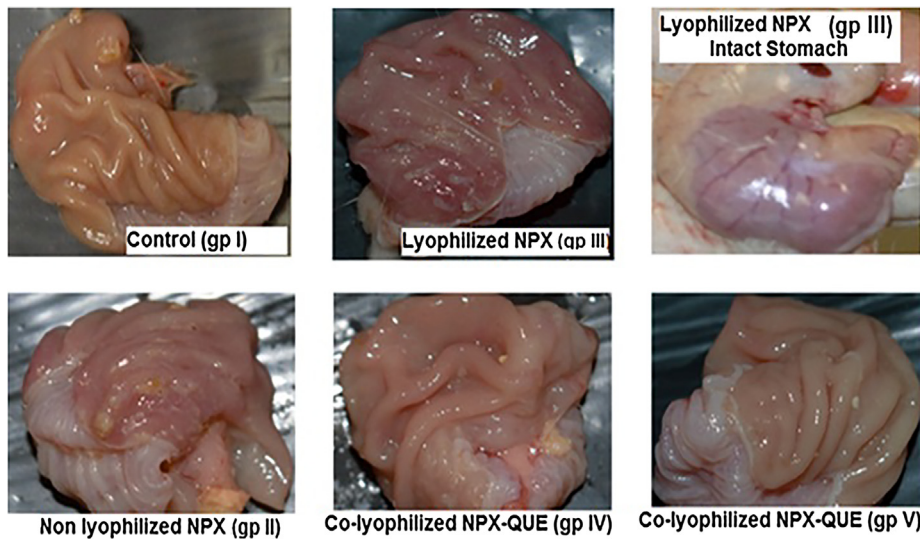

Fig.6. Representative macroscopic images of NXP-induced acute gastric mucosal injury and pretreatment with NPX-QUE co-lyophilizates.
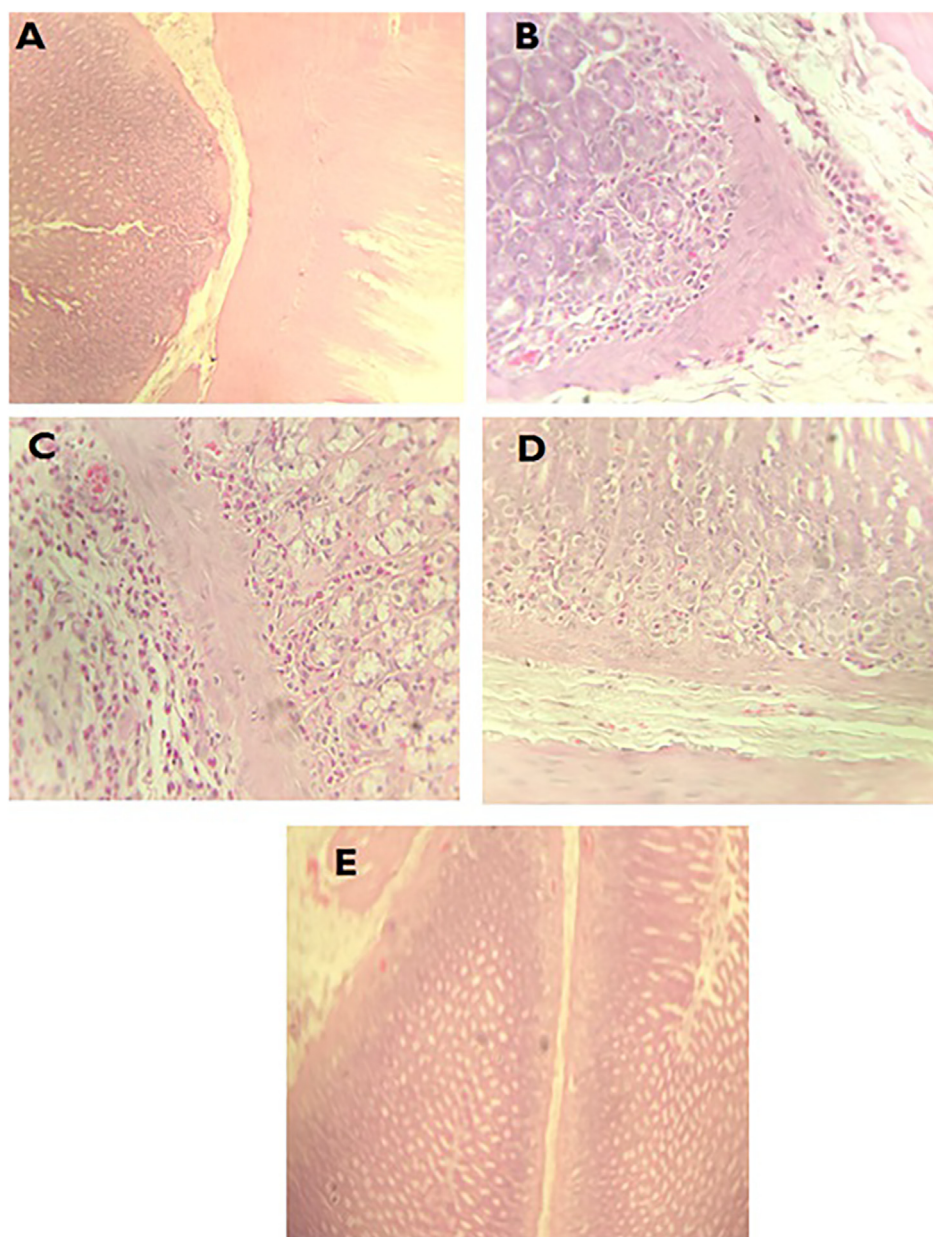
Fig. 7. Gastric biopsies stained by H& E showed no remarkable pathology gp I (A) (x100); moderate inflammatory cell infiltrated gp II (B) (x200; severe inflammatory cell infiltrated gp III (C) (x200); mild inflammatory cell infiltrated gp IV (D (x200)); no significant inflammatory cell infiltrated gp V (E) (x100).

was shown by mild leucocyte infiltration and edema in the submucosal layer, and less congested capillaries with no erosions (Fig. 7). Biopsies from group V did not show any significant leucocyte infiltration in the mucosa with very minimal edema (Fig. 7). The same results were obtained by Khaleel et al. (2015). In addition, Boots et al. (2008) showed that QUE has anti-inflammatory, antiproliferative, and neuroprotective effects, and protected normal and diabetic rats against indomethacin-induced gastric ulcers. The proinflammatory mediators and reduction of defensive mechanisms can be increased by NSAIDs (Hawkey and Langman, 2003). Moreover, Amić et al. (2017) demonstrated that QUE is an excellent free radical scavenging compound that might help in the reduction of the risk of oxidative stress related chronic diseases, such as inflammation and gastric irritation. This study proved that QUE Catholic colonic metabolites have the potential to deactivate various free radicals by direct scavenging via double sequential proton loss electron transfer (SPLET) and double atom transfer (AT)

mechanisms depending upon the polarity of the environment (Amić et al., 2017).

Table 2
The main pharmacokinetic parameters of NPX after oral administration of NPX-QUE 1:2 co-lyophilizate and untreated NPX in rats (n = 6).

Parameters	Untreated NPX	NPX-QUE 1: 2 co-lyophilizate
C_{max} (µg/ml)	187.93 ± 11.03	205.16 ± 11.09[*]
T_{max} (h)	4.0	2.0[*]
AUC_{0-24} (µg.h/ml)	1837.27 ± 96.58	1845.54 ± 54.71
AUC_{0-inf} (µg.h/ml)	2212.37 ± 82.18	2452.81 ± 115.28[*]
K_{el} (h)	0.086 ± 0.07	0.055 ± 0.008[*]
$t_{1/2}$ (h)	9.33 ± 0.77	12.73 ± 1.95[*]
MRT (h)	12.98 ± 1.80	16.93 ± 2.49[*]

Relative bioavailability: 100.45%.
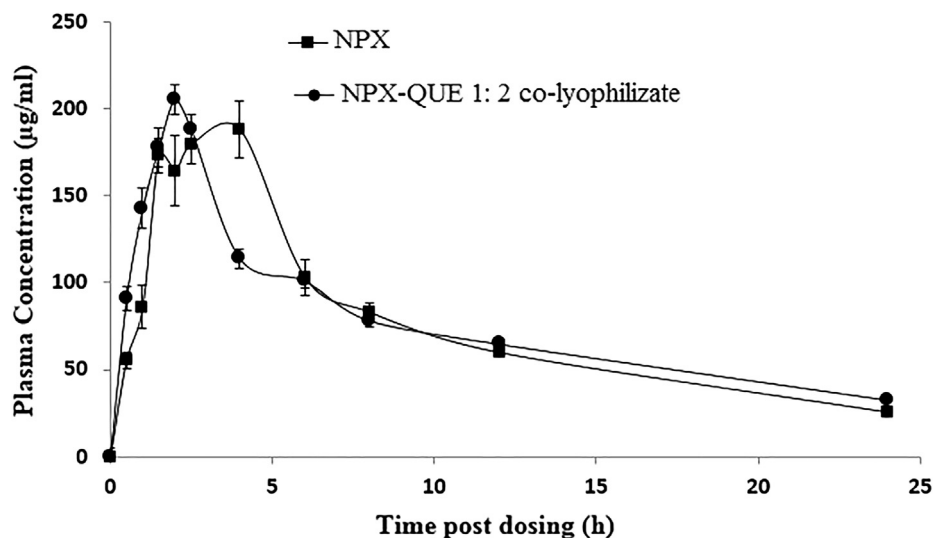[*] P < 0.05 significant compared with untreated NPX.

Fig. 8. Plasma concentration–time plots of NPX after oral administration of NPX-QUE co-lyophilizate and untreated NPX in rats (Mean ± SD; n = 6).

7. Pharmacokinetics

The bioavailability and pharmacokinetic studies were carried out to analyze the NPX contents in rat plasma after oral administration of untreated NPX and NPX-QUE 1:2 co-lyophilizate formulations.

The pharmacokinetic data of the two NPX formulations are presented in Table 2 and Fig. 8. The value of t_{max} was recorded at 2.0 h for NPX-QUE 1:2 co-lyophilizate and at 4.0 h for the untreated NPX. C_{max} was 187.93 ± 11.03 ng mL^{-1} for NPX-QUE 1:2 co-lyophilizate and 205.16 ± 11.09 ng mL^{-1} for untreated NPX. The difference in C_{max} between the two formulations was statistically significant ($P < 0.05$). The value of AUC$_{0–24}$ was recorded as $1837.27 \pm 96.58 \pm 11.03$ ng mL^{-1} and 1845.54 ± 54.71 ng mL^{-1} for NPX-QUE 1:2 co-lyophilizate and the untreated NPX, respectively. This difference was not statistically significant ($P < 0.05$). Moreover, AUC$_{0–\infty}$ of the NPX-QUE 1:2 co-lyophilizate and the untreated NPX were 2452.81 ± 115.28 ng h mL^{-1} and 2212.37 ± 82.18 ng h mL^{-1}, respectively, which were also statistically significant ($P < 0.05$). Furthermore, the relative bioavailability of NPX-QUE 1:2 co-lyophilizate with the untreated NPX was 100.45%. The shorter T_{max} and the higher C_{max} obtained in the NPX-QUE 1:2 co-lyophilizate were correlated with the enhanced drug dissolution rate, which resulted in rapid drug absorption with high plasma level. Junyaprasert and Morakul (2015) showed that when NPX was prepared as a nanosuspension (270 nm) by milling to enhance its dissolution rate for oral administration, the AUC of the drug from the nanosuspension was approximately 3-fold higher than that of the unmilled NPX suspension (20 μm). In addition, a reduced T_{max} and enhanced C_{max} were observed. These authors suggested that an increase in the drug bioavailability in the nanosuspension might be due to the increased solubility and dissolution rate of nanocrystals.

4. Conclusion

To improve the therapeutic efficacy of NPX as a NSAID member, improving the drug dissolution rate should be concomitant with minimizing its adverse reactions, especially GI ulceration. The results of the present study demonstrated that QUE co-lyophilization with NPX caused a remarkable improvement in the drug dissolution rate in the acidic medium. In addition, QUE combined with NPX resulted in enhanced pharmacokinetic parameters,

along with a protective effect on the stomachs of rats from NPX-induced inflammation.

References

Amić, A., Lučić, B., Stepanić, V., Marković, Z., Marković, S., Dimitrić Marković, J.M.5., Amić, D., 2017. Free radical scavenging potency of quercetin catecholic colonic metabolites: thermodynamics of 2H. Food Chem. 218, 144–151.

Boots, A.W., Haenen, G.R., Bast, A., 2008. Health effects of quercetin: from antioxidant to nutraceutical. Eur. J. Pharmacol. 585 (2–3), 325–337.

Carrasco-Pozo, C., Castillo, R.L., Beltrán, C., Miranda, A., Fuentes, J., Gotteland, M., 2016. Molecular mechanisms of gastrointestinal protection by quercetin against indomethacin-induced damage: role of NF-κB and Nrf2. J. Nutr. Biochem. 27, 289–298.

Carrasco-Pozo, C., Pastene, E., Vergara, C., Zapata, M., Sandoval, C., Gotteland, M., 2012a. Stimulation of cytosolic and mitochondrial calcium mobilization by indomethacin in Caco-2 cells: modulation by the polyphenols quercetin, resveratrol and rutin. Biochim. Biophys. Acta 1820, 2052–2061.

Carrasco-Pozo, C., Mizgier, M.L., Speisky, H., Gotteland, M., 2012b. Differential protective effects of QUE, resveratrol, rutin and epigallocatechin gallate against mitochondrial dysfunction induced by indomethacin in Caco-2 cells. Chem. Biol. Interact. 195, 199–205.

Chairmandurai, A.R., Kanappa, S.V., Vadrevu, K.M., Putcha, U.K., Venkatesanc, V., 2010. Recombinant human epidermal growth factor alleviates gastric antral ulcer induced by naproxen: a non-steroidal anti inflammatory drug. Gastroenterol. Res. 3, 125–133.

Dhikav, V., Singh, S., Pande, S., Chawla, A., Anand, K.S., 2003. Non-steroidal drug-induced gastrointestinal toxicity:mechanisms and management. J. Ind. Acad. Clin. Med. 4 (4), 315–322.

Elsinghorst, P.W., Kinzig, M., Rodamer, M., Holzgrabe, U., Sörgel, F., 2011. An LC-MS/MS procedure for the quantification of naproxen in human plasma: development, validation, comparison with other methods, and application to a pharmacokinetic study. J. Chromatogr. B Analyt Technol. Biomed. Life Sci. 19, 1686–1696.

Ghosh, R., Alajbegovic, A., Gomes, A.V., 2015. NSAIDs and cardiovascular diseases: role of reactive oxygen species. Oxid. Med. Cell Longev. 536962, 1–25.

Hawkey, C., Langman, M., 2003. Non-steroidal anti-inflammatory drugs: overall risks and management. Complementary roles for Cox-2 inhibitors and proton pump inhibitors. Gut 52, 600–608.

Junyaprasert, V.B., Morakul, B., 2015. Nanocrystals for enhancement of oral bioavailability of poorly water-soluble drugs. Asian J. Pharm. Sci. 10, 13–23.

Kayaçetin, S., Güreşçi, S., 2014. What is gastritis? What is gastropathy? How is it classified? Turk. J. Gastroenterol. 25, 233–247.

Khaleel, E.F., Mostafa, D.G., Abdel-Aleem, G.A., 2015. Gastroprotective effect of flavonoid quercetin and coenzyme Q10 in indomethacin-induced gastric ulcers in normal and diabetic rats. OSR J. Dent. Med. Sci. 14 (12), 58–71.

Kim, J.H., Kim, Y.S., Song, G.G., Park, J.J., Chang, H., 2005. Protective effect of astaxanthin on naproxen-induced gastric antral ulceration in rats. Eur. J. Pharmacol. 514 (1), 53–59.

Lain, L., 2002. The gastrointestinal effects of nonselective NSAIDs and COX-2–selective inhibitors. Semin. Arthr. Rheum. 32 (3), 25–32.

Materska, M., 2008. Quercetin and its derivatives: chemical structure and bioactivity-a review. Pol. J. Food Nutr. Sci. 58, 407–413.

Matsui, H., Shimokawa, O., Kaneko, T., Nagano, Y., Rai, K., Hyodo, I., 2011. The pathophysiology of non-steroidal anti-inflammatory drug (NSAID)-induced mucosal injuries in stomach and small intestine. J. Clin. Biochem. Nutr. 48 (2), 107–111.

Panahi, H.A., Feizbakhsha, A., Khaledia, S., Monir, E., 2013. Fabrication of new drug imprinting polymer beads for selective extraction of naproxen in human urine and pharmaceutical samples. Int. J. Pharm. 441, 776–780.

Rugge, M., Meggio, A., Pennelli, G., Piscioli, F., Giacomelli, L., De Pretis, G., Graham, D. Y., 2007. Gastritis staging in clinical practice: the OLGA staging system. Gut 56 (5), 631–636.

Scarpignato, C., Hunt, R.H., 2010. Nonsteroidal antiinflammatory drug-related injury to the gastrointestinal tract: clinical picture, pathogenesis, and prevention. Gastroenterol. Clin. North Am. 39, 433–464.

Schuna, A.A., Megeff, C., 2002. New drugs for the treatment of rheumatoid arthritis. Am. J. Health-Syst. Pharm. 57, 225–234.

Straube, S., Tramèr, M.R., Moore, R.A., Derry, S., McQuay, H.J., 2009. Mortality with upper gastrointestinal bleeding and perforation: effects of time and NSAID use. BMC Gastroenterol. 9, 41–47.

Vemula, S.K., Vangala, M., 2014. Formulation development and characterization of meclizine hydrochloride sublimated fast dissolving tablets. Int. Sch. Res. Notices 2014, 281376–281384.